0038-075C/02/16703-165–172
Soil Science

March 2002
Vol. 167, No. 3
Printed in U.S.A.

TECHNICAL ARTICLES

SOIL PORE SIZE AND GEOMETRY AS A RESULT OF AGGREGATE-SIZE DISTRIBUTION AND CHEMICAL COMPOSITION

I. Lebron[1], D.L. Suarez[1], and M.G. Schaap[1]

Soil pore size and pore geometry are important properties affecting soil hydraulic properties. Using scanning electron micrographs and image analysis, we quantified the actual pore-size distribution and pore shape in undisturbed soil cores. Aggregate-size distribution was also quantified for the same micrographs. For soils with similar texture, we observed a decrease both in the median aggregate size and in the aggregate-size distribution when the sodium content in the soil increased. We hypothesize that the decrease in the aggregate stability is caused by the weakening of the binding capacity of the cementing agents bonding the domains that form the aggregates. An equivalent decrease in the pore-size distribution was found with increasing sodium and pH. There was a significant correlation between median aggregate size and median pore size, but there was not a significant correlation between median pore diameter and soil texture. (Soil Science 2002;167:165–172)

Key words: Thin sections, scanning electron microscopy, image analysis, undisturbed soil samples.

SOIL pore space and its intrinsic characteristics such as surface area, roughness, tortuosity, and connectivity are probably the most important factors controlling water and solute movement in soils. Interaggregate porosity is the result of the arrangement of the soil aggregates. These aggregates are composed of subunits, of which clay minerals and other colloids are the main components. The way in which clay minerals and colloids arrange themselves determines the size and shape of the soil aggregates. Colloids are chemically and biologically very active, and this activity has been attributed to their high surface area and to the electric field surrounding the particles (Goldberg et al., 1999). The equilibrium distance between clays is the result of the forces caused by the electric field around the individual platelets, which results in a nonrandom arrangement of the particles in the soil. Properties at the mineral interface, together with the amount of water in the soil, control the type and strength of the association between particles. This self-arrangement is affected by chemical characteristics of the bulk solution, such as electrical conductivity (EC), type of cation, and pH.

In situations such as the reclamation of sodic soils or the use of drainage water for irrigation, the soil texture remains constant, but its chemical composition changes with time. Changes in chemical composition affect the size and stability of the aggregates and, consequently, the hydraulic properties of the soil. In order to model the chemically induced changes in hydraulic properties, we need to have an understanding of the processes involved. We also need a methodology that allows us to measure the stability of aggregates having varying chemical compositions. Traditional methodologies to quantify the aggregate stability are based on measuring the size of the

*Trade names are provided for the benefit of the reader and do not imply any endorsement by the USDA.

[1]USDA-Salinity Laboratory, 450 W. Big Springs Rd., Riverside, CA 92507-4617. Dr. Lebron is corresponding author. E-mail: ilebron@ussl.ars.usda.gov

Received July 27, 2001; accepted Nov. 27, 2001.

aggregates after the aggregates have been separated from the soil matrix, sieved through specific size screens, and submitted to cycles of immersion in water (Kemper and Rosenau, 1986). Unfortunately, results from laboratory experiments using disturbed soil samples overpredict the instability of the aggregates (Lebron et al., 2001). This overprediction is caused mainly because the natural structure of the soil, along with most of the natural aggregates, is often destroyed in the handling process.

Soil aggregates are created by the combination of one or more individual particles in a larger entity. This definition implies that the term "aggregate" applies to the microscopic scale and that aggregates form the building blocks of larger, possibly macroscopically observable, structures (such as aggregates in the pedological sense). Even at the microscopic scale, however, aggregates exist in different sizes. According to Tisdall and Oades (1982), the various aggregate fractions are formed as a result of the action of different stabilizing constituents. Aggregates smaller than 30 μm would be formed by oxides and microbial and fungal debris, encrusted mostly with clays. The aggregates 30 to 60 μm in size are considered to be stabilized by organic matter and inorganic minerals such as calcite. The silt-size particles and the aggregates larger than 60 μm are composites of larger mineral particles such as sand-size quartz, which are usually coated with oxides and often are associated with plant residues.

Although many experimental studies have measured changes in soil hydraulic properties with different sodium concentrations or different ionic strengths, few studies to date have measured the influence that these variables have on pore clogging, pore geometry, or pore-size distribution. There are also numerous studies about clay dispersion and soil aggregate stability in clean systems (Goldberg and Forster, 1990; Hesterberg and Page, 1990; Lebron and Suarez, 1992; Kretzschmar et al., 1993), but there is a gap in our knowledge of how this information can be put together to describe the interaction between the aggregates and the enclosed pores. To our knowledge, there are no data on direct measurement of aggregate-size distribution in undisturbed soil samples. Image analysis and microscopic techniques are two methodologies that may help us to cover this gap.

The objectives of the present study are: (i) to measure the aggregate- and pore-size distribution of undisturbed soil using thin sections, a microscopic technique, and image analysis; and (ii) to quantify the changes in aggregate and pore characteristics with changing chemical composition.

MATERIAL AND METHODS

We collected two sets of undisturbed soil samples from two fields in Coachella Valley, California. Each of the sets consists of eight 5-cm high by 5.5-cm diameter cores. The cores were collected by hand from the top 25 cm of the soil to avoid mechanical compression. The soil classifications are: Indio very fine sandy loam (samples 1–8) and Gilman silt loam (samples 9–16). The fields were monitored and mapped in a previous survey for electrical conductivity (EC) and sodium adsorption ratio (SAR) ($SAR = Na^{+}/(Ca^{2+}+Mg^{2+})^{0.5}$, where the cation concentration is expressed in mmol L^{-1}). A sampling scheme was established to cover a maximum range of EC and SAR. Disturbed samples were also collected from each site from which we collected the soil cores. The undisturbed cores were used to prepare the thin sections, and the disturbed samples were used to analyze for chemical composition and texture. The cation composition of the soil extracts was analyzed by inductively coupled plasma. Soil organic matter was determined by dry combustion (UIC Corp., Joliet, IL.)* Particle size distribution was measured following the methodology described in Gee and Bauder (1986).

The clay fraction (<2 μm) was collected from the soil samples of each of the two soil sets. X-ray diffractograms for mineral analysis were develop using a randomly oriented powder preparation and an oriented glass slide preparation, one with the clay sample saturated with potassium and the other with magnesium in 10% glycerol and 10% humidity (Whittig and Allardice, 1986).

Soil thin sections were prepared from the soil cores collected and observed in the scanning electron microscope (SEM). Thin sections were prepared by impregnation of the samples with epoxy EPO-TEK 301 (Epoxy Technology Inc., Billerica, MA). After hardening, a thin section 3.5 × 2.5 cm was cut at the plane perpendicular to the water flow, mounted on a glass slide, and polished. The polishing process was done with a series of diamond polishers to avoid the introduction of contaminants, and in the absence of water to preserve soluble minerals. Figure 1a shows the image of a thin section; the gray gradient is produced by the electron reflection of the components of the soil and is proportional to the atomic

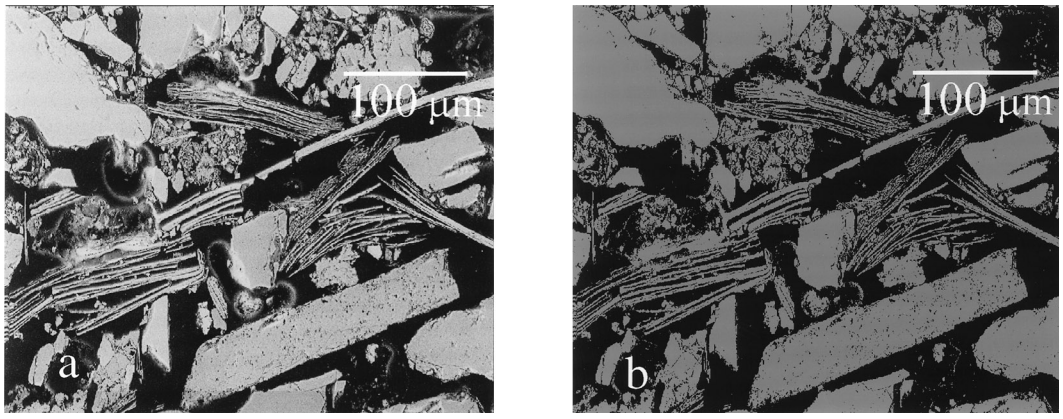

Fig. 1. a) Micrograph in grey scale of an undisturbed soil sample from Indio soil, Coachella Valley, CA. b) Same micrograph converted to a binary image using image analysis.

weight of the chemical element. This gray scale can be represented by a histogram with a bimodal distribution, which is used to resolve pores from particles through the transformation of the micrograph to a binary image. The histograms for the soils in this study presented an unambiguous minimum in between the two modes of the histograms, and we chose that mathematical minimum as the threshold to separate the pores and the particles. Figure 1b shows Fig. 1a transformed into a binary image.

The quantification of the features in the micropicture was performed using image analysis package software (Princeton Gamma-Tech Inc., Princeton, NJ). Once we have the binary image, the program proceeds to count the pixels that

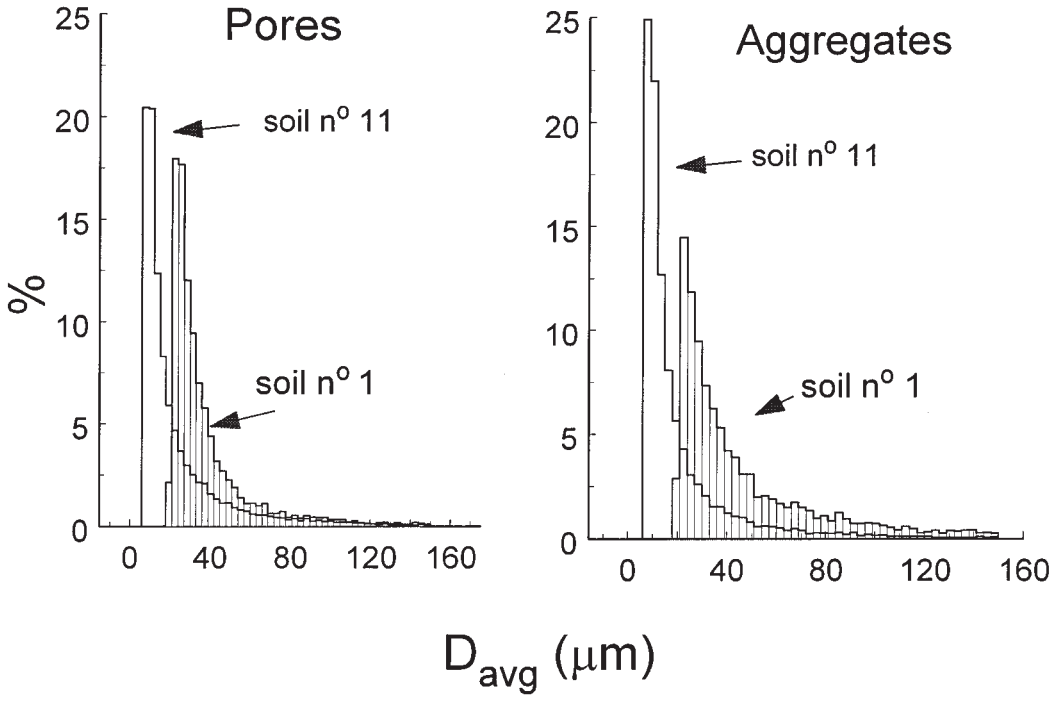

Fig. 2. Distribution of a) pore D_{avg} and b) aggregate D_{avg} measured in micrographs with image analysis for soils 1 and 11.

constitute each of the features: the bright pixels are the aggregates, and the dark pixels are the pores. Because our detection limit was already established to be 7 μm, we deemed that all of the bright features already constituted an aggregate. Average diameter (D_{avg}) was measured as the average of 12 directed diameters. The directed diameters are the projections of the pore or aggregate on 12 lines placed every 15° around a half-circle, starting with the x-axis as 0°. Moving counterclockwise, we measured the projections onto lines at 0, 15, 30, 45, 60, 75, 90, 105, 120, 135, 150, and 165°. D_{avg} was measured in each of the aggregates and pores in the micrographs. As shown in Fig. 2, the D_{avg} did not have a normal distribution in either the aggregates or in the pores; therefore, we used the median of the D_{avg} as the representative value for the aggregate and/or pore diameter for each sample.

Area (A) and perimeter (P) of pores and aggregates were also measured directly in the micrographs using the same image analysis. The medians of both parameters were used to express size and shape of pores or aggregates. Pore roughness (R) was expressed as $P/(\pi D_{avg})$.

Energy dispersive X-ray analysis (EDXA) was used to analyze the cementing material between the aggregates. This technique analyzes the X-ray radiation emanating from the specimen after bombarding it with the electron beam activated with the SEM. The analysis of the X-ray spectrum provides the chemical information for the sample. This chemical information can be selected from specific features or points in the picture and the accuracy is atomic weight dependent (Friel and Greenhut, 1999).

RESULTS AND DISCUSSION

Soil Pore Size and Geometry

The pore-size distribution of our samples varied greatly from one sample to the other. The change in the distribution of the pores was not caused exclusively by changes in texture, as changes in chemical composition were also important (Table 1). Increases in SAR had a considerable influence on the D_{avg} of the soil pores. Figure 3 shows the D_{avg} of the pores for each sample as a function of the SAR. Sodium adsorption ratio affected not only the median pore D_{avg} but also the pore-size distribution. Figure 2 shows the distribution for the totality of the pores (from 20,000 to 40,000) for Soils 1 and 11. We observed distinct differences in pore size aggregate distribution. Soils 1 and 11 were chosen because they have similar particle-size distribution and similar total porosity but very different SAR values. The D_{avg} of the pores also decreased when pH increased (Table 2).

Another parameter used frequently to describe the pore space is the hydraulic radius $(A/P)_p$, where A and P are the median of the area and perimeter measured in each of the pores of the micrograph (Lebron et al., 1999). In Table 2

TABLE 1

Particle size distribution, porosity measured with image analysis (φ_{SEM}) bulk density (ρ_B), electrical conductivity (EC), pH, and sodium adsorption ratio (SAR) of Indio silt loam and Gilman silt loam soils, Coachella Valley, CA

N⁰	Particles			φ_{SEM}	ρ_B	EC	pH	SAR
	<2 μm	2–50 μm	> 50 μm		g cm³	dS m⁻¹		
	%			%				
1	11.3	41.3	47.4	30.96	1.37	2.11	7.25	5.73
2	11.9	44.7	43.7	26.81	1.39	2.10	7.25	6.60
3	10.1	39.2	50.8	20.09	1.36	6.68	7.90	8.18
4	13.6	39.0	47.3	31.97	1.49	7.66	7.90	10.4
5	19.6	53.6	26.8	16.74	1.41	18.41	7.65	30.6
6	17.2	58.9	23.5	12.82	1.35	16.12	7.60	31.8
7	21.6	56.7	21.7	21.66	1.41	15.37	7.45	28.7
8	11.9	56.8	31.2	20.26	1.40	24.10	8.15	40.7
9	19.6	57.3	23.1	38.18	1.40	102.0	8.15	403
10	17.8	51.9	30.4	38.50	1.45	32.50	7.95	141
11	6.9	40.2	52.9	36.89	1.49	5.05	8.50	73.0
12	3.1	14.2	82.7	37.01	1.38	13.83	7.90	64.9
13	13.8	50.4	35.7	27.53	1.35	73.80	8.00	183
14	12.6	75.9	11.5	32.88	1.39	57.20	7.90	162
15	5.6	12.9	81.4	31.93	1.40	36.90	7.90	86.7
16	4.6	43.6	51.8	56.81	1.43	22.60	8.30	98.7

we observe that the hydraulic radius was correlated with sand and silt but was apparently not affected by the chemical composition.

The importance of the pore shape to the hydraulic properties of a soil has been shown by several authors, e.g., Philip (1977), Reeves and Celia (1996), and Tuller et al. (1999). The introduction of shape factors in transport modeling allows for a better description of the system and represents adsorption phenomena and capillary behavior more realistically. One way to express the pore shape is by dividing the area of the pore by the square of the perimeter (A/P^2) (Jongerius and Bisdom, 1981; Norton, 1987; Mason and Morrow, 1991; Tuller et al., 1999).

In Table 2 we see that the median of the geometry of the pores was correlated only with the roughness, but if we represent the histogram of the pore shape factor A/P^2 (Fig. 4), we can observe the differences among the types of pore shapes. Figure 4 shows Soils 12 and 14 as an example, but significant differences were observed among the rest of the soils as well (data not shown). We do not have enough information at this point to attribute these changes to differences in particle-size distribution or differences in chemical composition.

To understand why the chemical composition affects the pore-size distribution and possibly the pore shape as well, we must analyze the other component in the soil, the aggregates. From Fig. 1 we see that pores are the spaces enclosed between the aggregates. To quantify and understand the properties of the pores requires an understanding of the mechanisms controlling the stability of the aggregates.

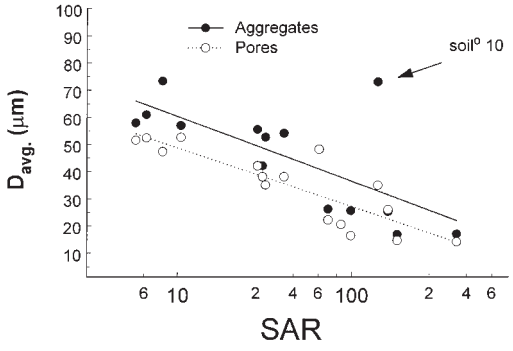

Fig. 3. Pore and aggregate D_{avg} as a function of sodium adsorption ratio (SAR) for Indio and Gilman soils, Coachella Valley, CA.

TABLE 2

Spearman rank correlation between variables porosity (Φ), pore median average diameter $(D_{avg})_P$, pore hydraulic radius (A/P), pore shape factor $(A/P^2)_p$, aggregate median average diameter $(D_{avg})_a$, aggregate A/P, aggregate shape factor $(A/P^2)_a$, pore roughness (R), electrical conductivity (EC), sodium adsorption ratio (SAR), pH, percentage of sand, silt and clay.
Numbers in bold are significant to p=0.005 and bold underlined are significant to p=0.0001.

	Φ	$(D_{avg})_P$	$(A/P)_p$	$(A/P^2)_p$	$(D_{avg})_a$	$(A/P)_a$	$(A/P^2)_a$	R	EC	SAR	pH	Sand	Silt	Clay
Φ	1													
$(D_{avg})_P$	−0.374	1												
$(A/P)_p$	0.318	0.400	1											
$(A/P^2)_p$	0.321	0.015	**0.677**	1										
$(D_{avg})_a$	−0.318	**0.621**	0.197	0.071	1									
$(A/P)_a$	**−0.697**	**0.694**	−0.065	0.021	**0.694**	1								
$(A/P^2)_a$	**−0.635**	0.171	0.032	0.112	−0.047	**0.597**	1							
R	0.314	−0.199	−0.329	**−0.582**	0.060	−0.279	**−0.642**	1						
EC	0.256	**−0.782**	−0.329	−0.024	**−0.577**	−0.294	−0.018	0.133	1					
SAR	**0.574**	**−0.885**	−0.306	0.032	**−0.671**	**−0.541**	−0.221	0.230	**0.862**	1				
pH	0.482	**−0.778**	−0.271	−0.085	−0.468	**−0.605**	−0.459	0.058	0.394	**0.635**	1			
Sand	0.271	0.141	**0.577**	0.141	−0.156	**−0.509**	−0.191	−0.172	−0.418	−0.182	0.126	1		
Silt	−0.227	−0.302	**−0.600**	−0.124	0.041	0.444	0.191	−0.034	0.453	0.297	−0.109	**−0.917**	1	
Clay	−0.311	−0.073	−0.497	−0.058	0.223	**0.556**	0.260	0.092	0.319	0.078	−0.326	**−0.880**	**0.683**	1

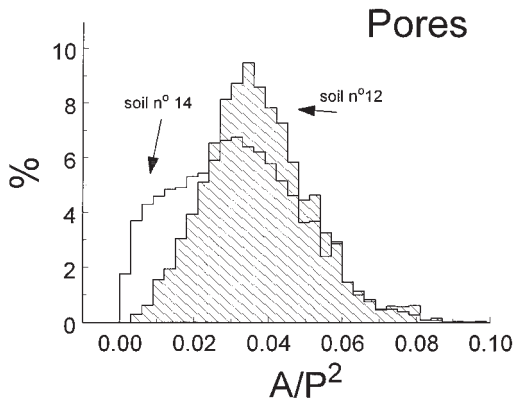

Fig. 4. Histogram for the pore shape factor expressed as area (A) divided by perimeter (P) square for two soils from Coachella Valley, CA.

Aggregate Size and Chemical Composition

The types of minerals present in a soil is a determining factor in the stability of soils (Goldberg and Forster, 1990). The clay mineral compositions found in both soil populations in this study were mica (di- and trioctahedral), kaolinite, and chlorite as the dominant clay minerals in that order, identified by the d-spacing listed in Fanning et al. (1989). Calcite and quartz were also detected, but neither smectite nor other swelling minerals were found. No significant changes in the distance between particles are expected since macroscopic swelling is not present in these soils; consequently, pore sizes and shapes are most likely not altered by wetting and drying processes. The organic matter content of the soils ranges from 0.8 to 1.3% of C (g/100g).

The soil samples were selected to study the chemical effects on soil aggregation, and, consequently, independence of chemical and physical properties was needed. There was no direct correlation between EC and texture or between SAR and texture for these samples (Table 2). There is a linear relationship between the SAR and EC, but this correlation is almost unavoidable in natural soils since values of EC above 5 to 10 dSm^{-1} are caused by the accumulation of highly soluble salts, and those salts are generally sodic in origin.

The D_{avg} of the aggregates decreased when the SAR increased (Fig. 3). Soils 12 and 15, shown in Table 1, are not shown in Fig. 3 because the different trend shown by these soils is most likely the result of the extremely high sand content. Since the mineralogy, organic matter content, and cementing agents are, in general, very similar for all the soils, we will consider the size of the aggregates as an indication of aggregate stability, similar to traditional aggregate stability tests. The decrease in aggregate size with increasing SAR is in agreement with data in the literature, where it is established that sodium has a deleterious effect on soil aggregate stability. More importantly, when we analyzed the aggregate-size distribution for each of the soils, we found a displacement toward smaller aggregates as SAR increased, similar to the results found for the pore-size distribution (Fig. 2). Soil 1, with lower sodium content (SAR=6), had larger aggregates than Soil 11 (SAR=73). The displacement of the aggregate-size distribution for Soil 1 with respect to Soil 11 is more than 30 μm.

Using an expression similar to that for hydraulic radius, we calculated the area divided by the perimeter (A/P) for aggregates. From Table 2 we observe that this parameter was correlated not only with the structural components of the soil, sand, and clay but also with the chemistry. The mechanisms involved in the process are not well understood. We hypothesize that the cementing agents acting as a glue among the quasicrystals are the main cause of aggregate destabilization when we increase the SAR or the pH.

Sodicity has an important role in the dispersion and flocculation of clay particles (Goldberg and Forster, 1990; Hesterberg and Page, 1990; Lebron and Suarez, 1992; Kretzschsmar et al., 1993), in the rearrangement of the platelets (Shainberg and Otho, 1968; Quirk and Aylmore, 1971; Lebron et al., 1993), and, consequently, in the hydraulic conductivity (Suarez et al., 1984). In the presence of elevated concentrations of sodium, the cementing agents that bridge the aggregates weaken their binding capability, and macro aggregates break apart. This breaking of the aggregates releases meso and micro plate-like aggregates that relocate in the pore space, redistributing the pore space into smaller pores.

As we can observe from the data scattering in Fig. 3, SAR is an important factor, but not the only one, affecting the size of the aggregates. For example, Soil 10 shows exceptionally high D_{avg} for a SAR of 141, indicating that other factors such as the pH and the amount of cementing material in the soils need to be examined. Figure 5 shows a cluster of clay domains. In between the plate-like entities that encompass the aggregate, we observe white crystals, identified with the EDXA probe as $CaCO_3$. The $CaCO_3$ precipitation most likely occurred during the succession

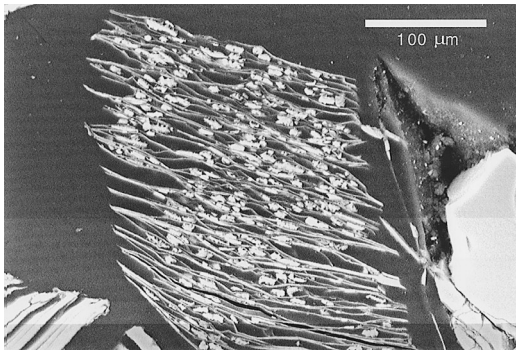

Fig. 5. Micrograph of a cluster of clay domains; calcite crystals can be observed in between the individual domains.

of wetting and drying processes that the soil has undergone since its development. The binding capacity of the calcite crystals is expected to change with changing external conditions. Partial pressure of CO_2, ionic strength, and pH also affect the surface speciation of the carbonate minerals. These chemical species may have a negative, positive, or neutral charge. In addition, dissolution and precipitation processes occur following the wetting and drying cycles. Other ubiquitous cementing materials are organic matter and iron and aluminum oxides, three compounds with different surface chemistries. There are several spectroscopic studies describing changes in the spatial configuration of organic molecules with varying ionic strength, pH, and cation composition (Danielsen et al., 1995, Green and Blough, 1996, Engebretson and von Wandruszka, 1998), but the nature of the interactions of organic matter with soil minerals is not well understood. More studies are needed to analyze the role of cementing agents in the stability of the aggregates.

The geometry of the aggregates was correlated with the roughness of the pores (Table 2). This may have important implications in hydraulic and transport processes.

Pore Space as a Function of Aggregate-Size Distribution

Arya and Paris (1981) presented a physical model of soil porosity based on particle-size distribution. In their model, the relation between the pore radius and particle radius involves an exponent that has subsequently been interpreted through a fractal concept (Tyler and Wheatcraft, 1989). Haverkamp and Parlange (1986) considered a constant packing parameter that relates pore and particle radii. Equally, the hydraulic parameters used in transport models and pedotransfer functions to predict water and solute transport in soils are very often based exclusively on texture and bulk density.

However, pores are the space enclosed between the soil aggregates: the larger the aggregates, the larger the pores, as shown in Fig. 6. No relationship was found between the pore D_{avg} and texture (Table 2), indicating that it is not the individual particles that determine the pore distribution but the association among the individual particles into highly ordered aggregates that disclose the open space where transport processes occur. Thus we expect that models to determine soil water properties will be more successful when they consider the aggregate and pore-space properties rather than just the texture and porosity. A model based on aggregates and porosity was developed by Rieu and Sposito (1991). Because the size of the aggregates is a function of the chemical composition, as we have shown above (Fig. 3), the relationship between the pore space and the chemical composition, is indirect but has immediate consequences in transport phenomena.

We conclude that pore size is determined by aggregate size (Fig. 6) and that aggregate size is affected by soil chemistry (Figs. 2 and 3, and Table 2). These conclusions are made possible by the use of image analysis and micrographs of soils where the structure has not been disrupted. Future studies will explore the determination of soil water properties using microscopic information combined with models that consider aggregate and pore space rather than models considering texture and porosity.

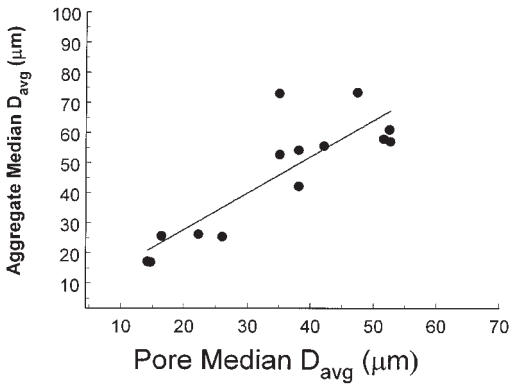

Fig. 6. Aggregate D_{avg} as a function of pore D_{avg}.

ACKNOWLEDGMENT

This study has been supported, in part, by NSF Grant EAR-007 4841.

REFERENCES

Arya, L. M., and J. F. Paris. 1981. A physico-empirical model to predict the soil moisture characteristic from particle-size distribution and bulk density data. Soil Sci. Soc. Am. J. 45:1023–1030.

Danielsen, K. M., Y. P. Chin, J. S. Buterbaugh, T. L. Gustafson, and S. Traina. 1995. Solubility enhancement and fluorescence quenching of pyrene by humic substances - The effect of dissolved oxygen on quenching processes. Environ. Sci. Technol. 29: 2162–2165.

Engebretson, R. R., and R. von Wandruszka. 1998. Kinetic aspects of cation-enhanced aggregation in aqueous humic acids. Environ. Sci. Technol. 32: 488–493.

Fanning, D. S., V. Z. Keramidas, and M. A. El-Desoky. 1989. Micas. *In* Minerals in Soil Environments, 2nd Ed. J.B. Dixon and S.B. Weed (eds.). SSSA and ASA, Madison, WI, pp. 551–634,

Friel, J. J., and V. A. Greenhut. 1999. Advances in X-ray microanalysis. Adv. Mater. Proc. 156:28–32.

Gee, G. W., and J. W. Bauder. 1986. Particle size analysis. *In* Methods of Soils Analysis, Part 1. Physical and Mineralogical Methods, Agron. Monogr. No. 9, 2nd Ed. A. Klute, (ed.). ASA, Madison, WI, pp. 383–412,

Goldberg, S., and H. S. Forster. 1990. Flocculation of reference clays and arid-zone soil clays. Soil Sci. Soc. Am. J. 54:714–718.

Goldberg, S., I. Lebron, and D. L. Suarez. 1999. Soil colloidal behavior. *In* Handbook of Soil Science. E. Sumner (ed.). CRC Press, Boca Raton, FL, pp. B195–240,

Green S. A., and N. V. Blough. 1996. Solubility enhancement and fluorescence quenching of pyrene by humic substances: The effect of dissolved oxygen on quenching processes (Comment). Environ. Sci. Technol. 30:1407–1408.

Haverkamp, R., and J. Y. Parlange. 1986. Predicting the water-retention curve from particle size distribution: 1. Sandy soils without organic matter. Soil Sci. 142:325–339.

Hesterberg, D., and A. L. Page. 1990. Critical coagulation concentration of sodium and potassium illite as affected by pH. Soil Sci. Soc. Am. J. 54:735–739.

Jongerius, A., and E. B. A. Bisdom. 1981. Porosity measurements using the Quantimet-720 on backscattered electron scanning images of thin sections of soils. *In* Submicroscopy of Soils and Weathered Rocks. E.B.A. Bisdom (ed.). Centre for Agric. Publ. and Doc., Wageningen, The Netherlands, pp. 207–216.

Kemper, W. D., and R. C. Rosenau. 1986. Aggregate Stability and Size Distribution. *In* Methods of Soil Analysis, Part 1, 2nd Ed. Agron. Monogr. 9. A. Klute (ed.). ASA and SSSA, Madison, WI, pp. 425–442.

Kretzschmar, R., W. P. Robarge, and S. B. Weed. 1993. Flocculation of kaolinitic soil clays: Effects of humic substances and iron oxides. Soil Sci. Soc. Am. J. 57:1277–1283.

Lebron, I., and D. L. Suarez. 1992. Variations in soil stability within and among soil types. Soil Sci. Soc. Am. J. 56:1412–1421.

Lebron, I., M. G. Schaap, and D. L. Suarez. 1999. Saturated hydraulic conductivity prediction from microscopic pore geometry measurements and neural network analysis, Water Resour. Res. 35:3149–3158.

Lebron, I., D. L. Suarez, C. Amrhein, and J. E. Strong. 1993. Size of mica domains and distribution of the adsorbed Na-Ca ions. Clays Clay Miner. 41:380–388.

Lebron, I., D. L. Suarez, and T. Yoshida. 2001. Gypsum effect on the aggregate size and geometry of three sodic soils under reclamation. Soil Sci. Soc. Am. J. 66:92–98.

Mason, G., and N. R. Morrow. 1991. Capillary behavior of a perfectly wetting liquid in irregular triangular tubes. J. Coll. Interface Sci. 141:262–274.

Norton, L. D. 1987. Micromorphological study of surface seals development under similated rainfall. Geoderma 40:127–140.

Philip, J. R. 1977. Adsorption and geometry: The boundary layer approximation. J. Chem. Phys. 67: 1732–1741.

Quirk, J. P., and L. A. G. Aylmore. 1971. Domains and quasi-crystalline regions in clay systems. Soil Sci. Soc. Am. Proc. 35:652–654.

Reeves, P. C., and M. A. Celia. 1996. A functional relationship between capillary pressure, saturation, and interfacial area as revealed by a pore-scale network model. Water Resour. Res. 32:2345–2358.

Rieu, M., and G. Sposito. 1991. Fractal fragmentation, soil porosity, and soil water properties: 1. Theory, Soil Sci. Soc. Am. J. 55:1231–1238.

Shainberg, I., and H. Otho. 1968. Size and shape of montmorillonite particles saturated with Na/Ca ions inferred from viscosity and optical measurements. Isr. J. Chem. 6:251–259.

Suarez, D. L., J. D. Rhoades, R. Lavado, and C. M. Grieve. 1984. Effect of pH on saturated hydraulic conductivity and soil dispersion, Soil Sci. Soc. Am. J. 48:50–55.

Tisdall, J. M., and J. M. Oades. 1982. Organic matter and water-stable aggregates in soils. J. Soil Sci. 33:141–163.

Tuller, M., D. Or, and L. M. Dudley. 1999. Adsorption and capillary condensation in porous media: Liquid retention and interfacial configurations in angular pores. Water Resour. Res. 35:1949–1964.

Tyler, S. W., and S. W. Wheatcraft. 1989. Application of fractal mathematics to soil water retention estimation. Soil Sci. Soc. Am. J. 53:987–996.

Whittig, L. D., and W. R. Allardice.1986. X-ray diffraction techniques. *In* Methods of Soil Analysis, Part 1. Physical and Mineralogical Methods. Agron. Monogr. No. 9, 2nd Ed. A. Klute (ed.). ASA, Madison, WI, pp. 331–362.